

# TRSM Benchmark Planes - Snowmass White Paper

Tania Robens<sup>1,\*</sup>

<sup>1</sup>*Ruder Boskovic Institute, Bijenicka cesta 54, 10000 Zagreb, Croatia*

(Dated: May 31, 2022)

## Abstract

In this whitepaper, I briefly review the Benchmark Planes in the Two-Real-Singlet Model (TRSM), a model that enhances the Standard Model (SM) scalar sector by two real singlets that obey a  $\mathbb{Z}_2 \otimes \mathbb{Z}'_2$  symmetry. In this model, all fields acquire a vacuum expectation value, such that the model contains in total 3 CP-even neutral scalars that can interact with each other. All interactions with SM-like particles are inherited from the SM-like doublet via mixing. I remind the readers of the previously proposed benchmark planes, and briefly discuss possible production at future Higgs factories.

arXiv:2205.14486v1 [hep-ph] 28 May 2022

---

\* trobens@irb.hr

## I. INTRODUCTION AND MODEL

The model discussed here has been proposed in [1], and I refer the reader to that reference for a detailed discussion of model setup and constraints. I just briefly repeat the generic features for completeness.

The potential in the scalar sector is given by

$$V(\Phi, S, X) = \mu_\Phi^2 \Phi^\dagger \Phi + \lambda_\Phi (\Phi^\dagger \Phi)^2 + \mu_S^2 S^2 + \lambda_S S^4 + \mu_X^2 X^2 + \lambda_X X^2 + \lambda_{\Phi S} \Phi^\dagger \Phi S^2 + \lambda_{\Phi X} \Phi^\dagger \Phi X^2 + \lambda_{SX} S^2 X^2. \quad (1)$$

Here,  $\Phi$  denotes the SM-like doublet, while  $X, S$  are two additional real scalar fields. The model obeys an additional  $\mathbb{Z}_2 \otimes \mathbb{Z}_2'$  symmetry  $\mathbb{Z}_2^S : S \rightarrow -S, \mathbb{Z}_2^X : X \rightarrow -X$ , while all other fields transform evenly under the respective  $\mathbb{Z}_2$  symmetry. All three scalars acquire a vacuum expectation value (vev) and therefore mix. This leads to three physical states with all possible scalar-scalar interactions.

Among the important constraints are e.g. the Higgs signal strength measurements by the LHC experiments, perturbative unitarity as well as the requirement for the potential to be bounded from below, and current collider searches. Results have been obtained using the `ScannerS` [2–6] framework. Experimental results from past and current collider experiments have been implemented using the publicly available tools `HiggsBounds` [7–12] and `HiggsSignals` [13–16].

In the following, we will use the convention that

$$M_1 \leq M_2 \leq M_3 \quad (2)$$

and denote the corresponding physical mass eigenstates by  $h_i$ . Gauge and mass eigenstates are related via a mixing matrix. Interactions with SM particles are then inherited from the scalar excitation of the doublet via rescaling factors  $\kappa_i$ , such that  $g_i^{h_i AB} = \kappa_i g_i^{h_i AB, \text{SM}}$  for any  $h_i AB$  coupling, where  $A, B$  denote SM particles. Orthogonality of the mixing matrix implies  $\sum_i \kappa_i^2 = 1$ . Furthermore, signal strength measurements require  $|\kappa_{125}| \gtrsim 0.96$  [1] for the SM-like scalar  $h_{125}$ , which can be  $h_1, h_2$  or  $h_3$  depending on the specific parameter choice.

For a certain production process (e.g. gluon gluon fusion) the cross section,  $\sigma$ , for  $h_a$  with mass  $M_a$  can be obtained from the corresponding SM Higgs production cross section,  $\sigma_{\text{SM}}$ , by simply rescaling

$$\sigma(M_a) = \kappa_a^2 \cdot \sigma_{\text{SM}}(M_a). \quad (3)$$

Since  $\kappa_a$  rescales all Higgs couplings to SM particles, Eq. (3) is exact up to genuine electroweak corrections involving Higgs self-interactions, and in particular holds to all orders in QCD.

The scaling factor  $\kappa_a$  plays the same role in universally rescaling the partial widths of  $h_a$  decays into SM particles, leading to

$$\Gamma(h_a \rightarrow \text{SM}; M_a) = \kappa_a^2 \cdot \Gamma_{\text{tot}}(h_{\text{SM}}; M_a), \quad (4)$$

where  $\Gamma(h_a \rightarrow \text{SM}; M_a)$  denotes the sum of all partial widths of  $h_a$  into SM particle final states. In addition, the branching ratios (BRs) of  $h_a$  decays to other scalar bosons,  $h_a \rightarrow h_b h_c$ , are given by:

$$\text{BR}(h_a \rightarrow h_b h_c) = \frac{\Gamma_{a \rightarrow bc}}{\kappa_a^2 \Gamma_{\text{tot}}(h_{\text{SM}}) + \sum_{xy} \Gamma_{a \rightarrow xy}}. \quad (5)$$

where the denominator now denotes the total width of the scalar  $h_a$ . In the absence of BSM decay modes — which is always the case for the lightest Higgs bosons  $h_1$  —  $h_a$  has BRs identical to a SM-like Higgs boson of the same mass.

## II. BENCHMARK PLANES

In [1], several benchmark planes were proposed which were meant to capture mainly features that by the time of that publication were not yet addressed by searches at the LHC:

- asymmetric production and decay, in the form of

$$p, p \rightarrow h_3 \rightarrow h_1 h_2,$$

where, depending on the kinematics,  $h_2 \rightarrow h_1 h_1$  decays are also possible;

- symmetric decays in the form of

$$pp \rightarrow h_i \rightarrow h_j h_j,$$

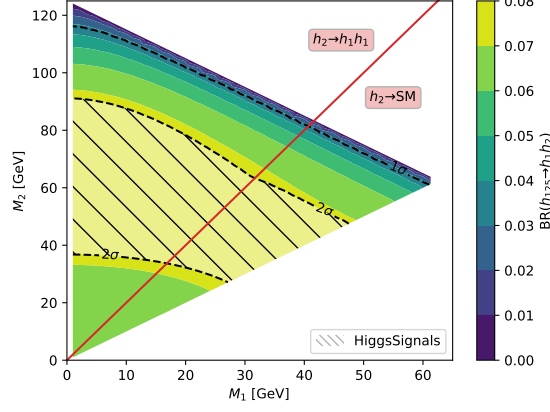
where none of the scalars corresponds to the 125 GeV resonance. Note that this in principle allows for further decays  $h_j \rightarrow h_k h_k$ , again depending on the specific benchmark plane kinematics.

We list the definition of these benchmark planes in tables I and II, respectively.

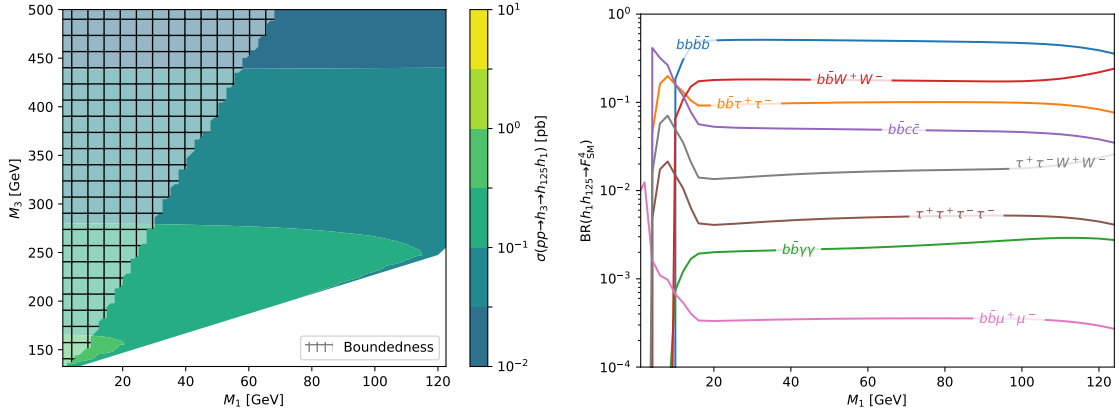
For this whitepaper, I rescanned all benchmark planes with the newest `HiggsBounds` and `HiggsSignals` versions: `HiggsBounds-5.10.2` and `HiggsSignals-2.6.2`. For nearly all parameter points, these new versions did not introduce additional constraints on the parameter space, and I therefore show the benchmark planes from the original publication. One exception is BP5 which has a slightly more constrained parameter space taking additional searches into account. I also comment on a possible recast on this plane and give a list of current experimental searches partially relying on our model.

### A. Asymmetric decays

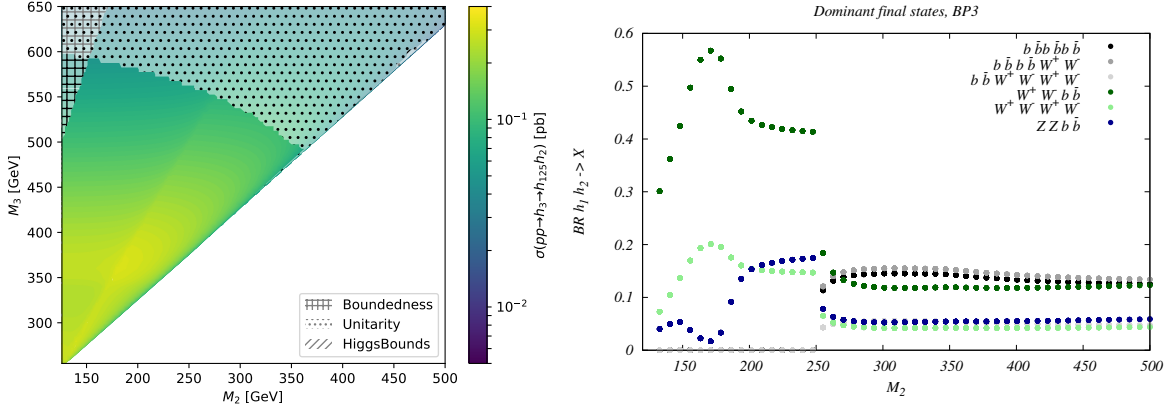
In this subsection, I discuss the asymmetric decay modes  $h_3 \rightarrow h_1 h_2$ , where successively one of the three scalars is identified with the 125 GeV resonance. I display the corresponding benchmark planes in figure 1.



Benchmark Plane 1



Benchmark Plane 2



Benchmark Plane 3

FIG. 1. Benchmark planes for asymmetric production and decay,  $pp \rightarrow h_3 \rightarrow h_1 h_2$ , for various assignments of the 125 GeV resonance. *Top row*: BP1, where  $h_3 \equiv h_{125}$ . Production cross sections are close to the SM production here, of around  $\sim 4$  pb at 13 TeV. Shown is the branching ratio to  $h_1 h_2$  in the two-dimensional mass plane. *Middle and bottom rows*: BPs 2 and 3, where  $h_{2,1} \equiv h_{125}$ , respectively. *Left*: Production cross sections at a 13 TeV LHC. *Right*: Branching ratios of the  $h_1 h_2$  state as a function of the free light scalar mass. Partially taken from [1].

benchmark scenario	$h_{125}$ candidate	target signature	possible successive decays
<b>BP1</b>	$h_3$	$h_{125} \rightarrow h_1 h_2$	$h_2 \rightarrow h_1 h_1$ if $M_2 > 2M_1$
<b>BP2</b>	$h_2$	$h_3 \rightarrow h_1 h_{125}$	-
<b>BP3</b>	$h_1$	$h_3 \rightarrow h_{125} h_2$	$h_2 \rightarrow h_{125} h_{125}$ if $M_2 > 250$ GeV
<b>BP4</b>	$h_3$	$h_2 \rightarrow h_1 h_1$	-
<b>BP5</b>	$h_2$	$h_3 \rightarrow h_1 h_1$	-
<b>BP6</b>	$h_1$	$h_3 \rightarrow h_2 h_2$	$h_2 \rightarrow h_{125} h_{125}$ if $M_2 > 250$ GeV

TABLE I. Overview of the benchmark scenarios: The second column denotes the Higgs mass eigenstate that we identify with the observed Higgs boson,  $h_{125}$ , the third column names the targeted decay mode of the resonantly produced Higgs state, and the fourth column lists possible relevant successive decays of the resulting Higgs states.

Parameter	Benchmark scenario					
	<b>BP1</b>	<b>BP2</b>	<b>BP3</b>	<b>BP4</b>	<b>BP5</b>	<b>BP6</b>
$M_1$ [GeV]	[1, 62]	[1, 124]	125.09	[1, 62]	[1, 124]	125.09
$M_2$ [GeV]	[1, 124]	125.09	[126, 500]	[1, 124]	125.09	[126, 500]
$M_3$ [GeV]	125.09	[126, 500]	[255, 650]	125.09	[126, 500]	[255, 1000]
$\theta_{hs}$	1.435	1.352	-0.129	-1.284	-1.498	0.207
$\theta_{hx}$	-0.908	1.175	0.226	1.309	0.251	0.146
$\theta_{sx}$	-1.456	-0.407	-0.899	-1.519	0.271	0.782
$v_s$ [GeV]	630	120	140	990	50	220
$v_x$ [GeV]	700	890	100	310	720	150
$\kappa_1$	0.083	0.084	0.966	0.073	0.070	0.968
$\kappa_2$	0.007	0.976	0.094	0.223	-0.966	0.045
$\kappa_3$	-0.997	-0.203	0.239	0.972	-0.250	0.246

TABLE II. Input parameter values and coupling scale factors,  $\kappa_a$  ( $a = 1, 2, 3$ ), for the six defined benchmark scenarios. The doublet vev is set to  $v = 246$  GeV for all scenarios.

Depending on the benchmark plane, maximal production cross sections are given by  $\sim 3 - 4$  pb,  $\sim 0.6$  pb, and 0.3 pb for  $h_1 h_2$  production for BPs 1/2/3, respectively. In BP3, the  $h_1 h_1 h_1$  final state reaches cross sections up to  $\sim 140$  fb. Note that as soon as the kinematic threshold for  $h_2 \rightarrow h_{125} h_{125}$  is reached, in fact decays from that state become dominant.

## B. Symmetric decays

Symmetric decays are given by BPs 4/5/6, with again a differing assignment for  $h_{3/2/1} \equiv h_{125}$ , respectively. The corresponding production and decay modes are displayed in figure 2.

Depending on the benchmark plane, pair-production cross sections can reach up to 60/ 2.5/ 0.5 pb for BPs 4/5/6, respectively. For the latter the  $h_{125}h_{125}h_{125}h_{125}$  final state can reach rates up to 14 fb. Also note that the allowed parameter space in BP5 has slightly shrunk, mainly due to the implementation of an additional search [17] into HiggsBounds after the performance of the original scan. For BP6, 6 particle final states as e.g.  $W^+W^-b\bar{b}b\bar{b}$  can reach branching ratios up to  $\sim 10\%$ , depending on  $M_2$ .

## III. FURTHER INVESTIGATION OF THIS MODEL

After the original appearance of the paper proposing the TRSM, several theoretical and experimental works have been performed which at least partially build on the benchmark planes proposed here. We briefly list some of these here.

### A. Investigation of the $h_{125}h_{125}h_{125}$ final state

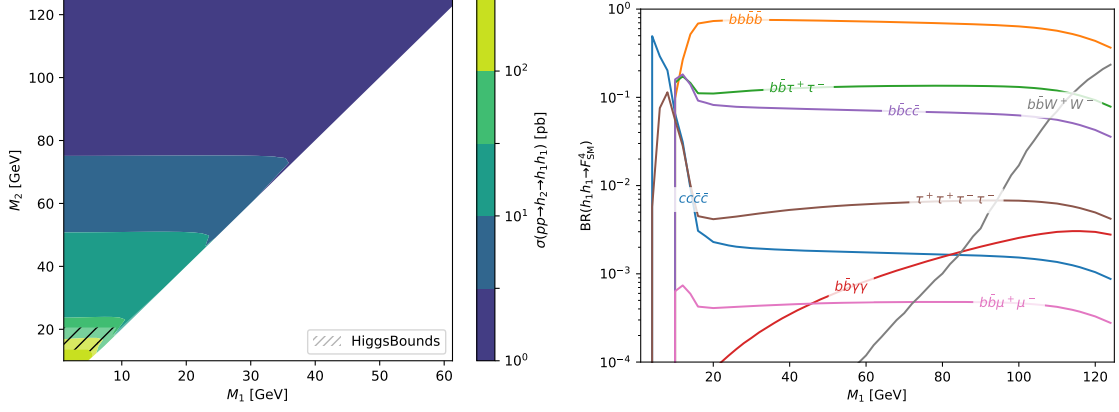
In BP3, for  $M_2 \rightarrow 250$  GeV, the decay  $h_2 \rightarrow h_1 h_1$  becomes dominant, leading to a  $h_{125}h_{125}h_{125}$  final state. For subsequent decays into  $b\bar{b}$ , this BP has been investigated in [18]. We found that, depending on the parameter point and integrated luminosity, significances between 3 and  $\sim 10$  can be achieved. We display the results in table III

Note we also compared how different channels, e.g. direct decays of the heavier scalars into  $VV$  or  $h_{125}h_{125}$  final states, would perform at a HL-LHC. The results are displayed in figure 3.

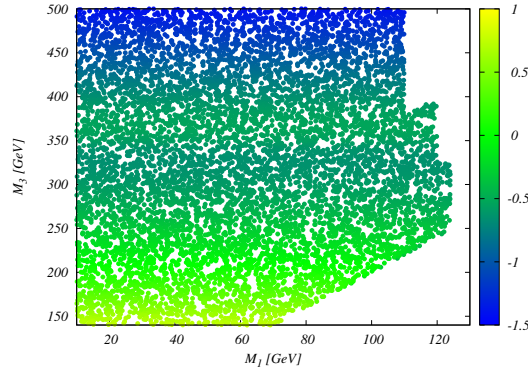
We note that all benchmark points that were investigated can additionally be probed by other production and decay mechanisms. Note, however, that these test different regions of the parameter space, as they depend on different parameters in the potential. These searches can therefore be considered to be complementary.

### B. Recasting current LHC searches

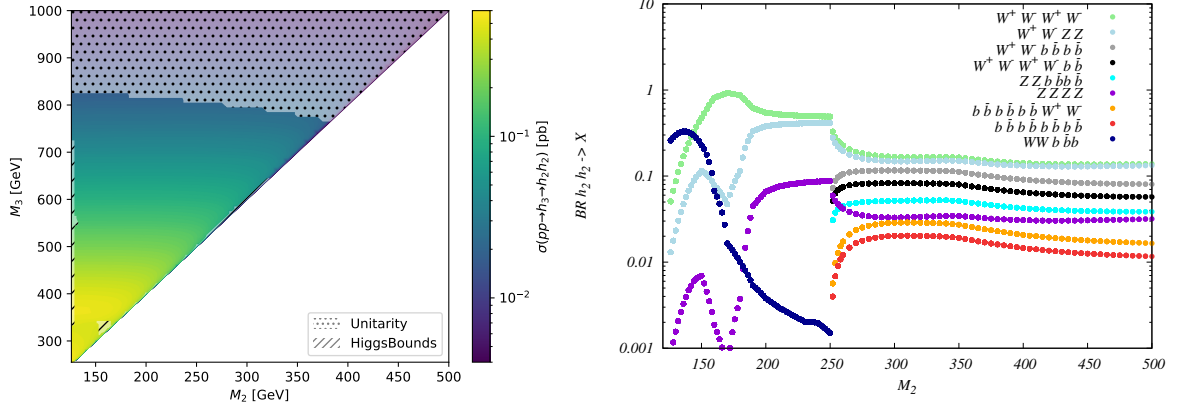
It is also interesting to investigate whether current searches can be reinterpreted and recasted in such a way that they allow to exclude regions in the models parameter space that were not directly scrutinized in the experimental search, or for which no interpretation was presented in the original publication. In [19], the authors have reinterpreted a CMS



Benchmark Plane 4



Benchmark Plane 5 [color coding:  $\log_{10}(\sigma_{h_3 \rightarrow h_1 h_1})$  [pb]]



Benchmark Plane 6

FIG. 2. Benchmark planes for symmetric production and decay,  $pp \rightarrow h_i \rightarrow h_j h_j$ , for various assignments of the 125 GeV resonance. *Top /middle/ bottom rows:* BPs 4/5/6, where  $h_{3/2/1} \equiv h_{125}$ . *Left:* Production cross sections at a 13 TeV LHC. *Right:* Branching ratios of the  $h_j h_j$  state as a function of the lighter free scalar mass. Branching ratios for BP4 and 5 are identical, therefore only one plot is displayed here. Partially taken from [1].

Label	$(M_2, M_3)$ [GeV]	$\varepsilon_{\text{Sig.}}$	$S _{300\text{fb}^{-1}}$	$\varepsilon_{\text{Bkg.}}$	$B _{300\text{fb}^{-1}}$	$\text{sig} _{300\text{fb}^{-1}}$ (syst.)	$\text{sig} _{3000\text{fb}^{-1}}$ (syst.)
<b>A</b>	(255, 504)	0.025	14.12	$8.50 \times 10^{-4}$	19.16	2.92 (2.63)	9.23 (5.07)
<b>B</b>	(263, 455)	0.019	17.03	$3.60 \times 10^{-5}$	8.12	4.78 (4.50)	15.10 (10.14)
<b>C</b>	(287, 502)	0.030	20.71	$9.13 \times 10^{-5}$	20.60	4.01 (3.56)	12.68 (6.67)
<b>D</b>	(290, 454)	0.044	37.32	$1.96 \times 10^{-4}$	44.19	5.02 (4.03)	15.86 (6.25)
<b>E</b>	(320, 503)	0.051	31.74	$2.73 \times 10^{-4}$	61.55	3.76 (2.87)	11.88 (4.18)
<b>F</b>	(264, 504)	0.028	18.18	$9.13 \times 10^{-5}$	20.60	3.56 (3.18)	11.27 (5.98)
<b>G</b>	(280, 455)	0.044	38.70	$1.96 \times 10^{-4}$	44.19	5.18 (4.16)	16.39 (6.45)
<b>H</b>	(300, 475)	0.054	41.27	$2.95 \times 10^{-4}$	66.46	4.64 (3.47)	14.68 (4.94)
<b>I</b>	(310, 500)	0.063	41.43	$3.97 \times 10^{-4}$	89.59	4.09 (2.88)	12.94 (3.87)
<b>J</b>	(280, 500)	0.029	20.67	$9.14 \times 10^{-5}$	20.60	4.00 (3.56)	12.65 (6.66)

TABLE III. The resulting selection efficiencies,  $\varepsilon_{\text{Sig.}}$  and  $\varepsilon_{\text{Bkg.}}$ , number of events,  $S$  and  $B$  for the signal and background, respectively, and statistical significances. A  $b$ -tagging efficiency of 0.7 has been assumed. The number of signal and background events are provided at an integrated luminosity of  $300 \text{ fb}^{-1}$ . Results for  $3000 \text{ fb}^{-1}$  are obtained via simple extrapolation. The significance is given at both values of the integrated luminosity excluding (including) systematic errors in the background. Taken from [18].

search for  $pp \rightarrow H \rightarrow h_{125}h_{125} \rightarrow 4b$  [20], which corresponds to di-Higgs production via a heavy resonance and subsequent decays into  $b\bar{b}$  final states, and extended the mass ranges for the scalars in the decay chain. I have applied these results to the TRSM, in particular to BP5. I display the corresponding results in figure 4<sup>1</sup>. We see that the sensitive region of parameter space is significantly extended, and therefore, an actual experimental analysis also in this parameter region is greatly encouraged.

### C. Experimental searches with TRSM interpretations

At least one experimental search actually has made use of the predictions obtained within the TRSM to interpret regions in parameter space that are excluded: a CMS search for asymmetric production and subsequent decay into  $b\bar{b}b\bar{b}$  final states [22]. For this, maximal production cross sections were provided in the parameter space, allowing all additional new physics parameter to float; the respective values have been tabulated in [23]. Figure 5 shows the expected and observed limits in this search for the TRSM and NMSSM [24].

<sup>1</sup> I thank the authors of [19] for providing us with the corresponding exclusion limits.

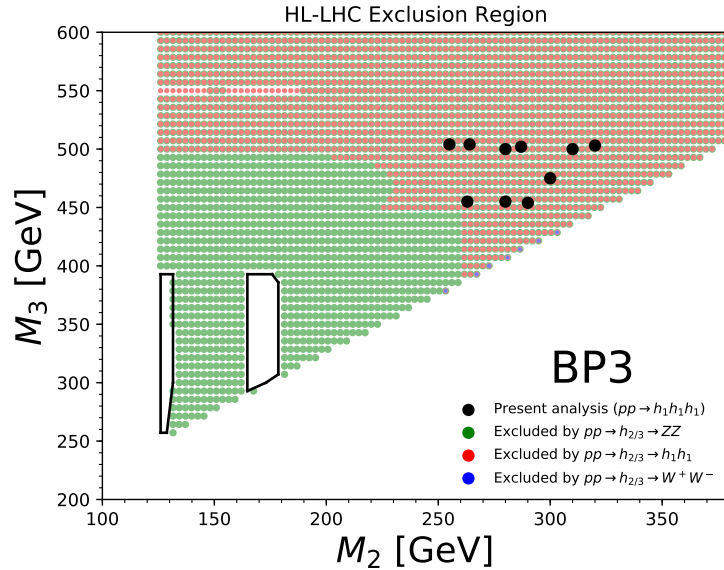


FIG. 3. The expected exclusion region for the full integrated luminosity of the HL-LHC,  $3000 \text{ fb}^{-1}$ , through final states *other* than  $pp \rightarrow h_1 h_1 h_1$  as explained in the main text. Points with green circles are expected to be excluded by  $ZZ$  final states, with red circles by  $h_1 h_1$  and with blue circles by  $W^+ W^-$ . The  $W^+ W^-$  analysis excludes only very few points on the parameter space and therefore appears infrequently in the figure. The points **A–I** that we have considered in our analysis of  $pp \rightarrow h_1 h_1 h_1$  are shown in black circles overlaid on top of the circles indicating the exclusion. The two cut-out white regions near  $M_2 \sim 130 \text{ GeV}$  and  $M_2 \sim 170 \text{ GeV}$  will remain viable at the end of the HL-LHC. Taken from [18].

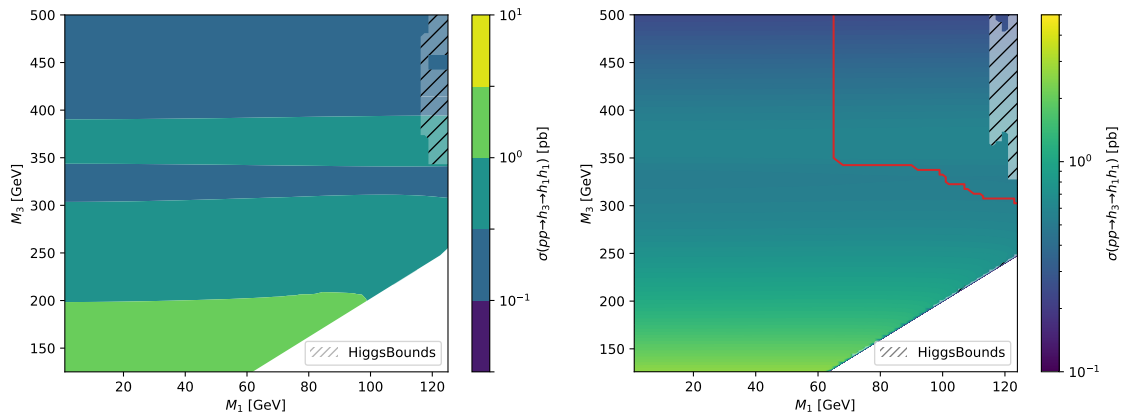


FIG. 4. Reinterpretation of a  $36 \text{ fb}^{-1}$  CMS search for di-Higgs production via a heavy resonance using the 4 b final state. The exclusion line uses the results obtained in [19]. Points to the right and above the red contour are excluded. Taken from [21].

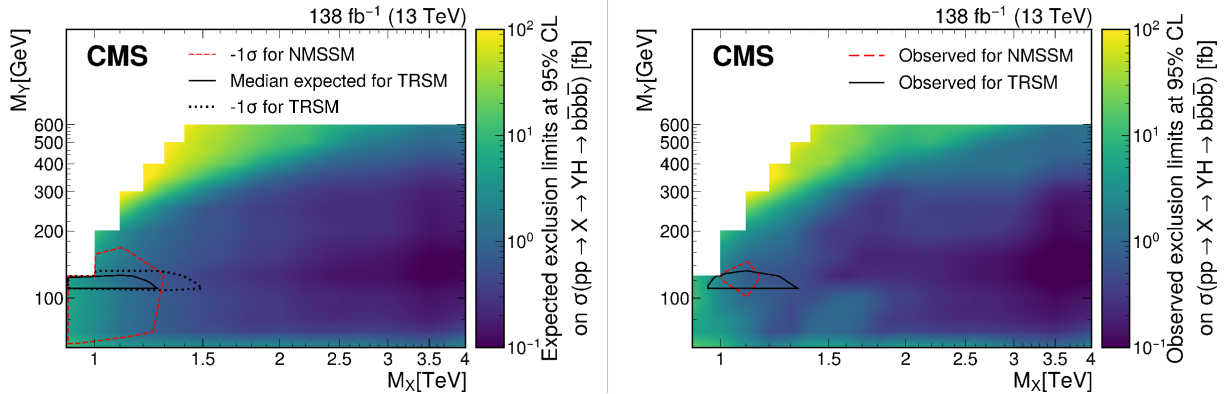


FIG. 5. Expected (*left*) and observed (*right*) 95% confidence limits for the  $pp \rightarrow h_3 \rightarrow h_2 h_1$  search, with subsequent decays into  $b\bar{b}b\bar{b}$ . For both models, maximal mass regions up to  $m_3 \sim 1.4\text{TeV}$ ,  $m_2 \sim 140\text{GeV}$  can be excluded. Figure taken from [22].

In addition, several searches also investigate decay chains that can in principle also be realized within the TRSM, as e.g. other searches for the same final states [25–27] or  $b\bar{b}\mu^+\mu^-$  [28, 29] final states.

#### IV. SIGNATURES AT HIGGS FACTORIES

The investigation of light scalars has recently gained again more interest, after the recommendation of the European Strategy Report [30, 31] to concentrate on  $e^+e^-$  machines with  $\sqrt{s} \sim 240 - 250\text{GeV}$ . A short review about the current state of the art for such searches and models which allow for low scalars can e.g. be found in [32]. In this model, the only feasible production is  $Zh$  radiation of the lighter scalar, with production cross sections given in figure 6. Cross sections have been derived using Madgraph5 [33].

We can now investigate what would be production cross sections for scalar particles with masses  $\lesssim 160\text{GeV}$  at Higgs factories.

##### A. Production of 125 GeV resonance and subsequent decays

We first turn to the easy case of the production of the 125 GeV resonance in various benchmark scenarios. Of interest are cases where decays  $h_{125} \rightarrow h_i h_j$  are kinematically allowed. Note that our benchmark points were not set up in particular for the scenario where  $i = j$ , so for this rates might be relatively small by construction.

From table II we see that for all scenarios the rescaling for the 125 GeV resonance is  $\gtrsim 0.966$ , leading to production cross sections of about  $\sim 0.2\text{pb}$ , close to the SM value. In general, due to constraints from the invisible branching ratio [34] as well as signal strength

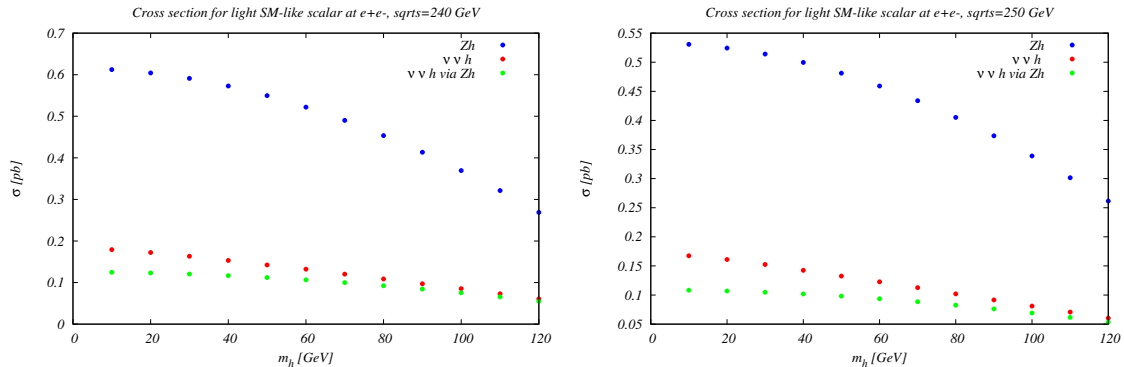


FIG. 6. Leading order production cross sections for  $Zh$  and  $h\nu_\ell\bar{\nu}_\ell$  production at an  $e^+e^-$  collider with a com energy of 240 GeV (*left*) and 250 GeV (*right*) using Madgraph5 for an SM-like scalar  $h$ . Shown is also the contribution of  $Zh$  to  $\nu_\ell\bar{\nu}_\ell h$  using a factorized approach for the  $Z$  decay. Taken from [32].

fits, the production cross section for  $h_i h_j$  final states has to be lower by at least an order of magnitude, leading to cross sections  $\mathcal{O}(10\text{fb})$ . In fact, in the benchmark planes presented here the largest rate for  $Zh_{125}$  production and subsequent scalar decays can be found in BP1, where the rates are given by multiplying the BRs from figure 1 with the production of  $Zh_{125}$ , giving maximal cross sections of around 18 fb.

## B. Additional scalar production

We now turn to the Higgs-Strahlung production of new physics scalars. This process is in principle possible in all BPs discussed here. However, if we require production rates of  $Zh_i$  to be larger than  $\sim 10\text{fb}$ , only BPs 4 and 5 render sufficiently large rates for the production of  $h_2$  and  $h_3$ , respectively. Production rates are independent of the other scalars, and we therefore depict them for both BPs in figure 7

BP4 is constructed in such a way that as soon as the corresponding parameter space opens up, the  $h_1 h_1$  decay becomes dominant; final states are therefore mainly  $Zb\bar{b}b\bar{b}$  if  $M_2 \gtrsim 2M_1$ . Below that threshold, dominant decays are into a  $b\bar{b}$  pair, which means that standard searches as e.g. presented in [35, 36] should be able to cover the parameter space.

Similarly, in BP5 the  $h_3 \rightarrow h_1 h_1$  decay is also favoured as soon as it is kinematically allowed. Therefore, in this parameter space again  $Zb\bar{b}b\bar{b}$  final states become dominant. Otherwise  $Zb\bar{b}$  and  $ZW^+W^-$  final states prevail, with a cross over for the respective final states at around  $M_3 \sim 135\text{GeV}$ . Branching ratios for these final states are in the 40 – 50% regime.

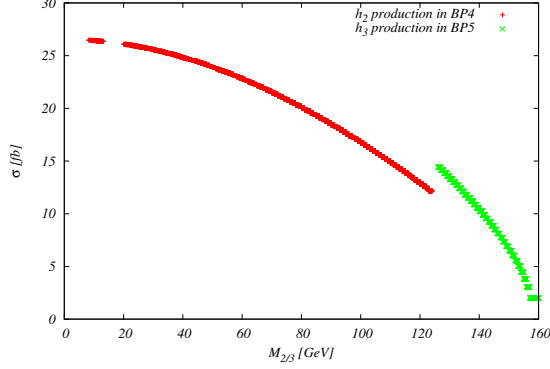


FIG. 7. Production cross sections for  $Zh_{2/3}$  in BPs 4 and 5, respectively, at a 250 GeV Higgs factory.

## V. SUMMARY

In this whitepaper, I gave a short summary of the status of collider signatures and searches in the TRSM introduced in [1]. I gave a summary on current state of the art and investigation, including further detailed collider studies, recasts, as well as current searches that use or are motivated in this model. I also gave a brief overview on channels within this model that might be testable at future  $e^+e^-$  machines, with a focus in Higgs factories with  $\sqrt{s} \sim 250$  GeV.

- 
- [1] Tania Robens, Tim Stefaniak, and Jonas Wittbrodt. Two-real-scalar-singlet extension of the SM: LHC phenomenology and benchmark scenarios. *Eur. Phys. J. C*, 80(2):151, 2020, 1908.08554.
  - [2] Rita Coimbra, Marco O. P. Sampaio, and Rui Santos. ScannerS: Constraining the phase diagram of a complex scalar singlet at the LHC. *Eur. Phys. J.*, C73:2428, 2013, 1301.2599.
  - [3] P. M. Ferreira, Renato Guedes, Marco O. P. Sampaio, and Rui Santos. Wrong sign and symmetric limits and non-decoupling in 2HDMs. *JHEP*, 12:067, 2014, 1409.6723.
  - [4] Raul Costa, Margarete Mühlleitner, Marco O. P. Sampaio, and Rui Santos. Singlet Extensions of the Standard Model at LHC Run 2: Benchmarks and Comparison with the NMSSM. *JHEP*, 06:034, 2016, 1512.05355.
  - [5] Margarete Mühlleitner, Marco O. P. Sampaio, Rui Santos, and Jonas Wittbrodt. The N2HDM under Theoretical and Experimental Scrutiny. *JHEP*, 03:094, 2017, 1612.01309.
  - [6] Margarete Mühlleitner, Marco O. P. Sampaio, Rui Santos, and Jonas Wittbrodt. ScannerS: parameter scans in extended scalar sectors. *Eur. Phys. J. C*, 82(3):198, 2022, 2007.02985.
  - [7] Philip Bechtle, Oliver Brein, Sven Heinemeyer, Georg Weiglein, and Karina E. Williams. HiggsBounds: Confronting Arbitrary Higgs Sectors with Exclusion Bounds from LEP and the

- Tevatron. *Comput. Phys. Commun.*, 181:138–167, 2010, 0811.4169.
- [8] Philip Bechtle, Oliver Brein, Sven Heinemeyer, Georg Weiglein, and Karina E. Williams. HiggsBounds 2.0.0: Confronting Neutral and Charged Higgs Sector Predictions with Exclusion Bounds from LEP and the Tevatron. *Comput. Phys. Commun.*, 182:2605–2631, 2011, 1102.1898.
- [9] Philip Bechtle, Oliver Brein, Sven Heinemeyer, Oscar Stal, Tim Stefaniak, Georg Weiglein, and Karina Williams. Recent Developments in HiggsBounds and a Preview of HiggsSignals. *PoS, CHARGED2012:024*, 2012, 1301.2345.
- [10] Philip Bechtle, Oliver Brein, Sven Heinemeyer, Oscar Stål, Tim Stefaniak, Georg Weiglein, and Karina E. Williams. HiggsBounds – 4: Improved Tests of Extended Higgs Sectors against Exclusion Bounds from LEP, the Tevatron and the LHC. *Eur. Phys. J. C*, 74(3):2693, 2014, 1311.0055.
- [11] Philip Bechtle, Sven Heinemeyer, Oscar Stal, Tim Stefaniak, and Georg Weiglein. Applying Exclusion Likelihoods from LHC Searches to Extended Higgs Sectors. *Eur. Phys. J. C*, 75(9):421, 2015, 1507.06706.
- [12] Philip Bechtle, Daniel Dercks, Sven Heinemeyer, Tobias Klingl, Tim Stefaniak, Georg Weiglein, and Jonas Wittbrodt. HiggsBounds-5: Testing Higgs Sectors in the LHC 13 TeV Era. *Eur. Phys. J. C*, 80(12):1211, 2020, 2006.06007.
- [13] Oscar Stål and Tim Stefaniak. Constraining extended Higgs sectors with HiggsSignals. *PoS, EPS-HEP2013:314*, 2013, 1310.4039.
- [14] Philip Bechtle, Sven Heinemeyer, Oscar Stål, Tim Stefaniak, and Georg Weiglein. *HiggsSignals*: Confronting arbitrary Higgs sectors with measurements at the Tevatron and the LHC. *Eur. Phys. J. C*, 74(2):2711, 2014, 1305.1933.
- [15] Philip Bechtle, Sven Heinemeyer, Oscar Stål, Tim Stefaniak, and Georg Weiglein. Probing the Standard Model with Higgs signal rates from the Tevatron, the LHC and a future ILC. *JHEP*, 11:039, 2014, 1403.1582.
- [16] Philip Bechtle, Sven Heinemeyer, Tobias Klingl, Tim Stefaniak, Georg Weiglein, and Jonas Wittbrodt. HiggsSignals-2: Probing new physics with precision Higgs measurements in the LHC 13 TeV era. *Eur. Phys. J. C*, 81(2):145, 2021, 2012.09197.
- [17] Morad Aaboud et al. Search for pair production of Higgs bosons in the  $b\bar{b}b\bar{b}$  final state using proton-proton collisions at  $\sqrt{s} = 13$  TeV with the ATLAS detector. *JHEP*, 01:030, 2019, 1804.06174.
- [18] Andreas Papaefstathiou, Tania Robens, and Gilberto Tetlalmatzi-Xolocotzi. Triple Higgs Boson Production at the Large Hadron Collider with Two Real Singlet Scalars. *JHEP*, 05:193, 2021, 2101.00037.
- [19] D. Barducci, K. Mimasu, J. M. No, C. Vernieri, and J. Zurita. Enlarging the scope of resonant di-Higgs searches: Hunting for Higgs-to-Higgs cascades in  $4b$  final states at the LHC and future colliders. *JHEP*, 02:002, 2020, 1910.08574.

- [20] Albert M. Sirunyan et al. Search for resonant pair production of Higgs bosons decaying to bottom quark-antiquark pairs in proton-proton collisions at 13 TeV. *JHEP*, 08:152, 2018, 1806.03548.
- [21] Tania Robens. Models with (broken)  $Z_2$  symmetries. *PoS, DISCRETE2020-2021*:063, 2022, 2202.09636.
- [22] Search for a massive scalar resonance decaying to a light scalar and a Higgs boson in the four b quarks final state with boosted topology. 4 2022, 2204.12413.
- [23] Tania Robens.  $b\bar{b}b\bar{b}$  final states in the TRSM for asymmetric production and decay. <https://twiki.cern.ch/twiki/pub/LHCPhysics/LHCHWG3EX/rep.pdf>.
- [24] Ulrich Ellwanger and Cyril Hugonie. Benchmark planes for Higgs-to-Higgs decays in the NMSSM. *Eur. Phys. J. C*, 82(5):406, 2022, 2203.05049.
- [25] Search for a massive scalar resonance decaying to a light scalar and a Higgs boson in the four b quark final state with boosted topology. 2021.
- [26] Search for new particles in an extended Higgs sector in the four b quark final state at  $\sqrt{s} = 13$  TeV. 2021.
- [27] Armen Tumasyan et al. Search for new particles in an extended Higgs sector with four b quarks in the final state at  $\sqrt{s} = 13$  TeV. 3 2022, 2203.00480.
- [28] Search for Higgs boson decays into two spin-0 particles in the  $bb\mu\mu$  final state with the ATLAS detector in  $pp$  collisions at  $\sqrt{s} = 13$  TeV. 3 2021.
- [29] Georges Aad et al. Search for Higgs boson decays into a pair of pseudoscalar particles in the  $bb\mu\mu$  final state with the ATLAS detector in  $pp$  collisions at  $\sqrt{s}=13$  TeV. *Phys. Rev. D*, 105(1):012006, 2022, 2110.00313.
- [30] Richard Keith Ellis et al. Physics Briefing Book: Input for the European Strategy for Particle Physics Update 2020. 10 2019, 1910.11775.
- [31] European Strategy Group. 2020 Update of the European Strategy for Particle Physics. Technical report, Geneva, 2020.
- [32] Tania Robens. A short overview on low mass scalars at future lepton colliders. *Universe*, 8:286, 2022, 2205.09687.
- [33] Johan Alwall, Michel Herquet, Fabio Maltoni, Olivier Mattelaer, and Tim Stelzer. MadGraph 5 : Going Beyond. *JHEP*, 06:128, 2011, 1106.0522.
- [34] Combination of searches for invisible Higgs boson decays with the ATLAS experiment. Technical report, CERN, Geneva, Oct 2020. All figures including auxiliary figures are available at <https://atlas.web.cern.ch/Atlas/GROUPS/PHYSICS/CONFNOTES/ATLAS-CONF-2020-052>.
- [35] P. Drechsel, G. Moortgat-Pick, and G. Weiglein. Prospects for direct searches for light Higgs bosons at the ILC with 250 GeV. *Eur. Phys. J. C*, 80(10):922, 2020, 1801.09662.
- [36] Yan Wang, Mikael Berggren, and Jenny List. ILD Benchmark: Search for Extra Scalars Produced in Association with a  $Z$  boson at  $\sqrt{s} = 500$  GeV. 5 2020, 2005.06265.